Oncogene (2002) 21, 5117–5126

www.nature.com/onc

DNA binding and 3′–5′ exonuclease activity in the murine alternatively-spliced p53 protein

Zippora Shakked*[,1], Michael Yavnilovitch[1], A Joseph Kalb (Gilboa)[1], Naama Kessler[1], Roland Wolkowicz[2], Varda Rotter[2] and Tali E Haran*[,3]

[1]*Department of Structural Biology, Weizmann Institute of Science, Rehovot 76100, Israel;* [2]*Department of Molecular Cell Biology, Weizmann Institute of Science, Rehovot 76100, Israel;* [3]*Department of Biology, Technion, Haifa 32000, Israel*

In this study we show that the naturally occurring C-terminally alternative spliced p53 (referred to as AS-p53) is active as a sequence-specific DNA binding protein as well as a 3′–5′-exonuclease in the presence of Mg^{2+} ions. The two activities are positively correlated as the sequence-specific DNA target is more efficiently degraded than a non-specific target. In contrast, a mutated AS-p53 protein that is deficient in DNA binding lacks exonuclease activity. The use of modified p53 binding sites, where the 3′-phosphate is replaced by a phosphorothioate group, enabled the inhibition of DNA degradation under the binding conditions. We demonstrate that AS-p53 interacts with its specific DNA target by two distinct binding modes: a high-affinity mode characterized by a low-mobility protein-DNA complex at the nanomolar range, and a low-affinity mode shown by a high-mobility complex at the micromolar range. Comparison of the data on the natural and the modified p53 binding sites suggests that the high-affinity mode is related to AS-p53 function as a transcription factor and that the low-affinity mode is associated with its exonuclease activity. The implications of these findings to a specific cellular role of AS-p53 are discussed.
Oncogene (2002) **21,** 5117–5126. doi:10.1038/sj.onc.1205667

Keywords: alternatively-spliced p53; DNA binding; exonuclease activity; phosphorothioate-modified DNA-binding sites

Introduction

The tumor suppressor protein p53 and its relation to human cancer have been studied extensively during the past 20 years (for recent reviews see Levine, 1997; Wang and Harris, 1997; May and May, 1999; Ryan *et al*., 2001). In normal cells p53 is expressed in extremely low amounts due to a very short half-life of the protein. However, under various cellular stress situations, such as exposure to DNA damaging agents, endogenous wild type p53 is activated (Giaccia and Kastan, 1998; Jayaraman and Prives, 1999; Okorokov and Milner, 1999; Oren, 1999). This results in the accumulation of high levels of stabilized, biochemically altered p53 protein, initiating a cascade of events leading to a cell cycle arrest or to apoptosis, thus preventing the fixation of deleterious mutations in the genome.

p53 function is directly related to its ability to act as a transcriptional activator, mediated through sequence-specific binding to several DNA targets in the genome. The consensus DNA binding site is comprised of two decameric repeats of the general form: PuPuPuC(A/T)(A/T)GPyPyPy separated by 0–13 base pairs (El-Deiry *et al*., 1992; Funk *et al*., 1992). Genetic and biochemical approaches have been used to assign four major structural/functional domains (reviewd by Ko and Prives, 1996; May and May, 1999). The N-terminus contains a transactivation domain. This is the site of interaction of several proteins that activate or inhibit p53 activity as a transcription factor. The central core region contains a sequence-specific DNA binding domain. This domain contains four evolutionarily conserved regions where 80–90% of the missense mutations, identified in human tumors, are found (Hainaut *et al*., 1997; Hainaut and Hollstein, 2000). The C-terminus contains an oligomerization domain. The extreme C-terminus is a basic region, which was shown to bind DNA non-specifically and to regulate p53 sequence-specific binding (reviewed by Wolkowicz and Rotter, 1997; Ahn and Prives, 2001).

In addition to its DNA binding capacity, the p53 central core domain was shown to have an intrinsic 3′-5′ exonuclease activity (Mummenbrauer *et al*., 1996) that is modulated by alterations in the C-terminus (Janus *et al*., 1999). This exonuclease activity has been suggested to be involved in DNA damage repair (Albrechtsen *et al*., 1999).

An alternatively spliced variant of p53 was found in mouse (referred to as AS-p53), in which the last 26 amino acids of the regularly spliced p53 (RS-p53) are replaced by 17 different residues (Arai *et al*., 1986; Han and Kulesz-Martin, 1992). AS-p53 was shown to exist in both non-transformed and malignant epidermal

*Correspondence: Z Shakked and TE Haran;
E-mail: zippi.shakked@weizmann.ac.il or bitali@techunix.technion.ac.il
Received 9 January 2002; revised 30 April 2002; accepted 10 May 2002

cells, and to be localized in the nucleus (Kulesz-Martin *et al*., 1994). The cellular level of AS-p53 is tissue and cell cycle phase specific (Kulesz-Martin *et al*., 1994). AS-p53 is expressed in normal cells at about 25% of the level of RS-p53 (Han and Kulesz-Martin, 1992). Cells expressing AS-p53 are detected preferentially in the G2 phase of the cell cycle, whereas RS-p53 is expressed primarily in cells that are in the G1 phase (Han and Kulesz-Martin, 1992).

The two proteins were also found to be functionally different. It was shown that AS-p53 induced a p53-dependent apoptosis that is significantly attenuated in comparison to that induced by RS-p53 (Almog and Rotter, 1997). Whereas the C-terminal domain of RS-p53 was shown to promote the reassociation of single-stranded RNA or DNA into duplex hybrids, the C-terminal domain of AS-p53 did not have this annealing capacity (Wu *et al*., 1995). More recently, it was found that AS-p53 exhibited a negative effect on the activity of RS-p53 in cells co-expressing both forms, thus suggesting that the expression of the C-terminally altered protein serves as another mechanism for controlling p53 cellular function (Almog *et al*., 2000). AS-p53 produced in bacteria or by *in vitro* translation has been shown to be constitutively active for sequence-specific DNA binding under conditions where RS-p53 required activation (Wu *et al*., 1994; Wolkowicz *et al*., 1995).

In this study we characterize the DNA binding and exonuclease activity of the alternatively spliced mouse p53. We show that this protein exhibits a high level of $3'-5'$ exonuclease activity in the presence of Mg^{2+} ions, and that DNA binding and exonuclease activity are correlated. To distinguish DNA binding from exonuclease activity we used modified oligonucleotides that are not susceptible to enzymatic degradation by AS-p53. We find that AS-p53 binds to its specific DNA targets in two different modes. The implications of these findings to a specific cellular role of AS-p53 that is distinct from that of RS-p53 are discussed.

Results

Production of p53 variants in E. coli

A quantitative characterization of sequence-specific DNA binding of proteins should preferably be carried out on homogeneous protein samples such as those produced in bacteria. AS-p53 produced in *E. coli* was found to bind sequence-specifically to its DNA target (Wolkowicz *et al*., 1995). Hence, we focus on the bacterially produced AS-p53 and its single-mutated form Cys129Phe (M8-p53), in our attempts to characterize protein-DNA interactions in this system. Under conditions used for expression, most of the protein accumulated in inclusion bodies (see experimental section). We have been able to solubilize the proteins and obtain pure and monodisperse protein samples (Figure 1). The bacterially produced wt AS-p53 was active with respect to DNA binding (see below).

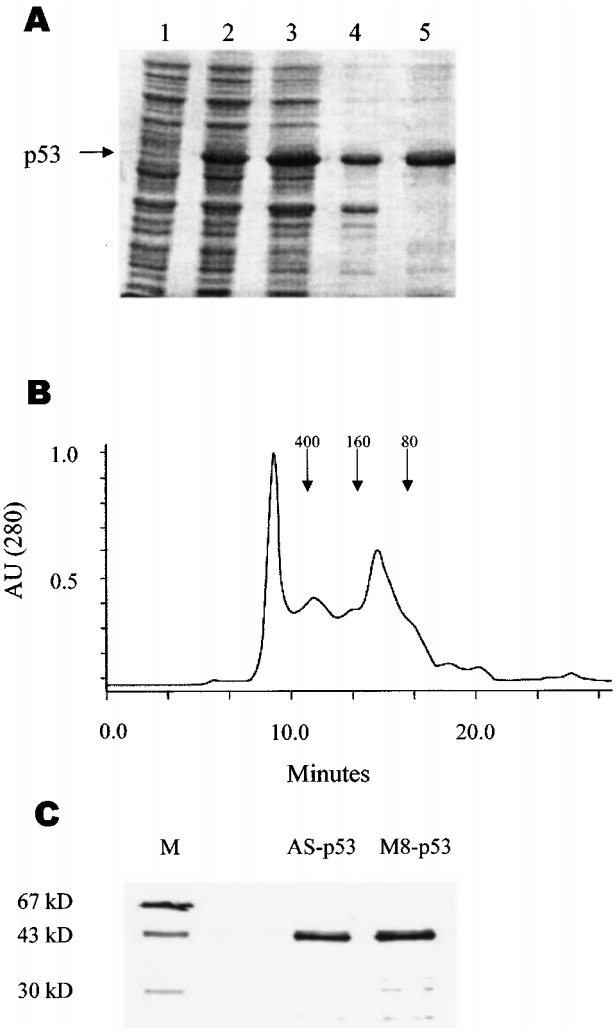

Figure 1 (**a**) A Coomassie stained SDS gel showing the isolation of AS-p53 from inclusion bodies. Lane 1: whole cell after bacterial growth to OD_{600} of 0.7, lane 2: after induction with 0.4 mM IPTG for 4 h, lane 3: after extensive sonication of the cells, lane 4: washed pellet, lane 5: after refolding from urea and dialysis into buffer as in Materials and methods. (**b**) Gel filtration chromatography of AS-p53 after refolding using Superdex 200-HR column (Pharmacia). The arrows show retention times for oligomeric proteins with the corresponding molecular weights (in kD units). (**c**) A Silver stained SDS gel of AS-p53 and M8-p53 after the final purification step (see Materials and methods)

DNA binding to AS-p53

The first step in characterizing the sequence-specific binding of AS-p53 to its DNA target was to find the optimal conditions for this interaction. To achieve this goal, several parameters were varied including the sequence of the DNA target, binding buffers, mono- and divalent cations, additives (e.g., glycerol, non-ionic detergents and DTT), the temperature of incubation of the protein-DNA mixture and that for running the gel, gel running buffer and gel composition. The DNA sequences used in our experiments are presented in Figure 2. Each DNA target incorporates two decameric repeats constituting sequence-specific p53

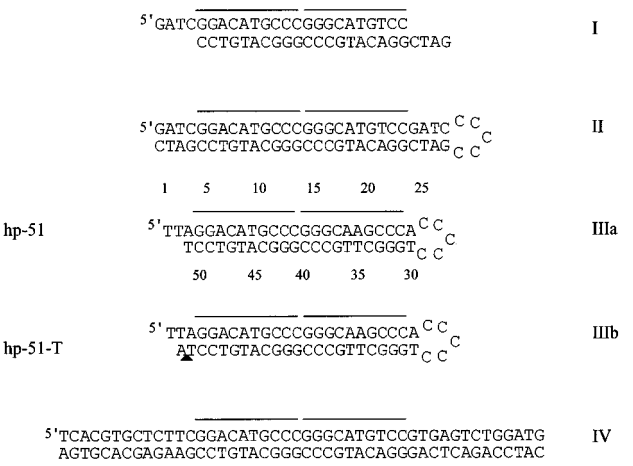

Figure 2 DNA sequences used in this study. The p53 binding sites (highlighted by lines) of sequences I, II, and IV are from Funk *et al.* (1992), and that of III is from Zauberman *et al.* (1993). Sequences II, IIIa and IIIb are hairpin constructs, where the double-stranded stem is connected by a loop of 5 cytosines (see text for details). Sequence IIIb has a phosphorothioate group at the 3′ end marked by a triangle. The numbering of nucleotides of sequence IIIa is from the 5′ to the 3′ end corresponding to the length of the oligonucleotide shown in Figure 5

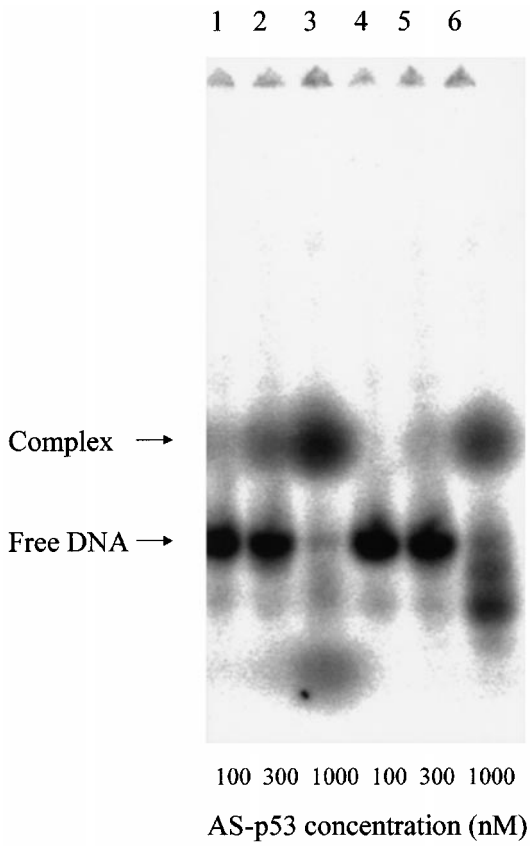

Figure 3 Band-shift pattern of AS-p53 bound to hp-51. Reaction mixtures were incubated for 70 min (lanes 1–3) and for 15 min (lanes 4–6). The bands below the arrow marking free DNA are degradation products (see text). The DNA concentration is 0.5 nM. Here and in the following figures the phosphor storage plate images of the gel electrophoretograms are shown

binding sites (Funk *et al.*, 1992; Zauberman *et al.*, 1993). The double-stranded DNA targets were contained within a linear duplex or a hairpin-looped construct, with either sticky or blunt ends. Mg^{++} ions were found essential for a quantitative gel shift for all sequences with an optimal concentration of 2.5 mM. In the absence of Mg^{++} ions a quantitative band shift could be obtained only with the long double-stranded construct (sequence IV of Figure 2) but the complexes were unstable and tended to dissociate during the electrophoretic run (data not shown). Very weak binding of the protein to the DNA was achieved in the presence of 1 mM Mn^{++} ions, whereas other divalent cations (e.g., 1–10 mM Ca^{++} or Zn^{++}) failed to promote efficient AS-p53 binding to any of the DNA constructs (data not shown).

The data presented below were obtained by using a 51 oligonucleotide with a 22 base pair double-stranded stem and a 5 base single-stranded loop (sequence IIIa in Figure 2, referred to as hp-51), unless indicated otherwise. The advantage of using a hairpin construct in cases of palindromic DNA binding sites is that it avoids uncertainty in the stability and concentration of the free DNA in its active double-helical form (Haran *et al.*, 1992).

In several of our initial DNA binding experiments (Figure 3), the shifted bands were broad and diffuse. A change from sharp bands to unusually smeared bands also appeared at the free DNA regions as the protein concentration was increased. In the experiment shown in Figure 3 the protein-DNA mixture was incubated for either 70 min (lanes 1–3) or 15 min (lanes 4–6). The multiple and smeared band patterns at the position of the free DNA showed that the DNA was progressively degraded as a function of time (compare lanes 3 and 6 of Figure 3). Smeared bands were also observed for the other DNA constructs (data not shown). This finding indicated that the DNA was degraded by the protein under the binding conditions. This phenomenon was observed previously for RS-p53 by Deppert and coworkers (Mummenbrauer *et al.*, 1996) who concluded that the protein acts as a 3′–5′-exonuclease under certain conditions. We therefore proceeded to look into the possibility of the exonucleolytic activity of AS-p53 as described below.

3′–5′ exonuclease activity of AS-p53

To test the possibility of DNA digestion by AS-p53, the protein and the DNA components were incubated under the conditions detailed in the experimental section, and then the pattern of DNA digestion was analysed as a function of incubation time. The DNA patterns shown in Figure 4 demonstrate that the DNA target was rapidly digested by AS-p53 in the presence of 2.5 mM $MgCl_2$. We checked the direction of digestion by labeling sequence I at either end. The degradation pattern of DNA labeled at its 5′-end

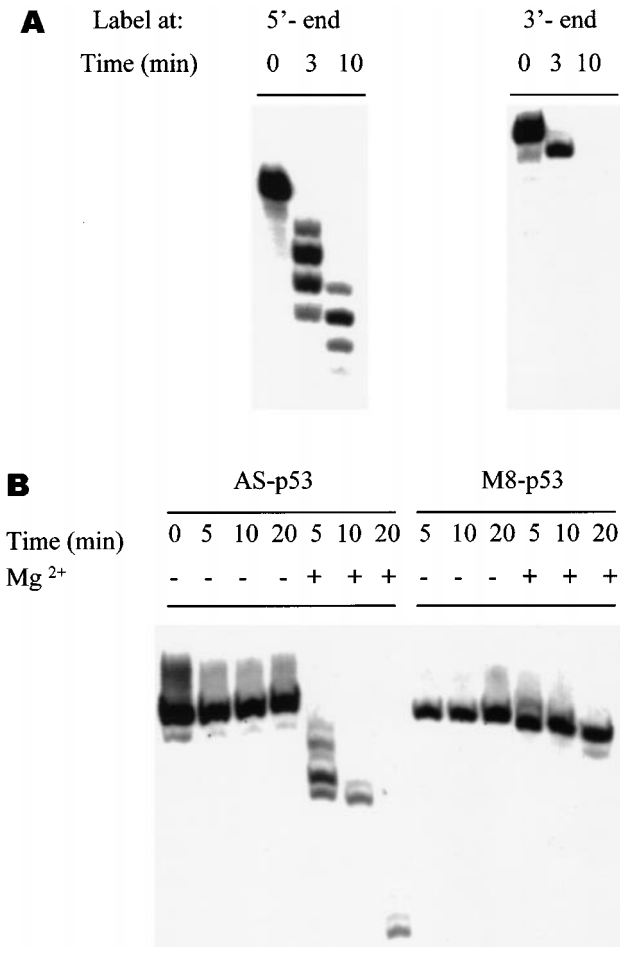

Figure 4 Exonuclease activity of p53 variants. (**a**) DNA degradation of sequence I by AS-p53 using 5′-end labeling (left panel) and 3′-end labeling (right panel) in the presence of 2.5 mM Mg^{++}. (**b**) DNA degradation as a function of time by AS-p53 (left panel) and M8-p53 (right panel) in the absence and presence of Mg^{++}. Lane 1 is a control lane without any protein. The level of radioactivity decreases as a function of time because the labeled nucleotides run out of the gel. The experiments were conducted by using 500 nM protein with 0.5 nM DNA labeled at the 5′-end (**b**) and either 5′- or 3′-labeled DNA in (**a**) (see Materials and methods)

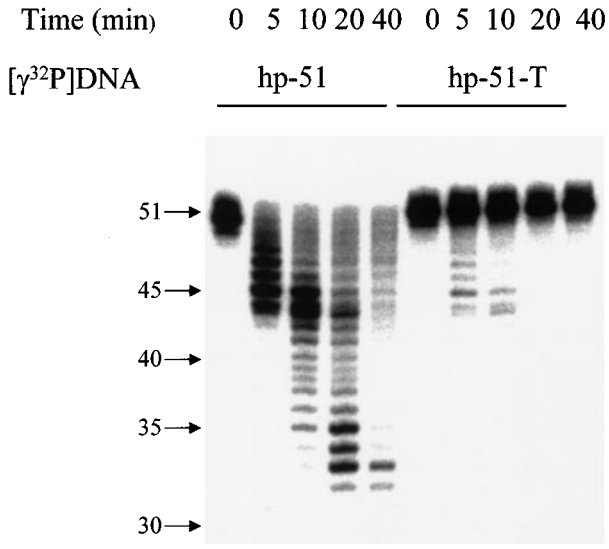

Figure 5 Exonuclease activity of AS-p53 protein on the natural sequence, hp-51 (sequence IIIa), versus the phosphorothioate analogue of this sequence, hp-51-T (sequence IIIb). 500 nM protein and 0.5 nM DNA were used in each experiment, as detailed in Materials and methods. The numbers at the left panel correspond to the size of the oligonucleotide fragments where the first lane from the left shows the band of the intact 51-mer DNA

showed a ladder of bands whereas the one labeled at the 3′-end showed only two bands (Figure 4a). Since sequence I was elongated by dGTP, [α-^{32}P]dATP and dTTP, the two bands correspond to the intact 27 oligonucleotide and the 26 oligonucleotide where the 3′-terminal thymine nucleotide has been removed. This observation demonstrates that cutting proceeded from the 3′-end as previously observed for the regularly spliced wild type p53 (Mummenbrauer *et al*., 1996). The effect of divalent ions is shown in Figures 4b by the patterns obtained for sequence IIIa. The presence of Mg^{2+} ions is essential for the exonuclease activity of AS-p53 as also shown previously for RS-p53. In the absence of divalent cations this activity was dramatically reduced. The 3′-5′ exonuclease activity was reproducible with several independent AS-p53 preparations. In contrast to the wild type AS-p53, the mutant protein, M8-p53, lacking DNA binding activity and prepared by an identical procedure as the natural protein, did not exhibit significant exonuclease activity (Figure 4b). Thus, we propose that wild type AS-p53 has an intrinsic 3′-5′ exonuclease activity as shown for RS-p53 (Mummenbrauer *et al*., 1996; Janus *et al*., 1999).

To characterize the mode of AS-p53/DNA interaction, a homogeneous DNA target is required. Thus, it was necessary to inhibit DNA degradation under the binding conditions. Dideoxynucleotide residues at the 3′-end of the DNA target were shown to inhibit degradation by some exonucleases (Longley and Mosbaugh, 1991). However, no significant influence on DNA degradation of such oligonucleotides by AS-p53 was observed (data not shown). Oligonucleotides with a phosphorothioate group at the 3′-end are known to dramatically decrease the efficiency of several exonucleases (Eckstein, 1985). Steitz and coworkers studied the structural basis of 3′-5′-exonuclease activity using the Klenow fragment of DNA polymerase I as a model system (Brautigam and Steitz, 1998). Two isomers are formed in the synthesis of a phosphorothioate oligonucleotide, referred to as R_p and S_p (see Figure 2 by Brautigam and Steitz, 1998). These authors found that the catalyzed hydrolysis of the R_p isomer was reduced by about 15-fold, whereas no enzymatic activity could be detected with the S_p phosphorothioate, consistent with the structural observations (Brautigam and Steitz, 1998).

We synthesized a p53 binding site identical to that of hp-51 (oligonucleotide IIIa in Figure 2), except for an additional adenine base at the 3′-end and a phosphorothioate modification at the potentially scissile

phosphate group at that end (oligonucleotide IIIb in Figure 2). We refer to this DNA as hp-51-T. Figure 5 shows a comparison between the degradation of the natural and modified DNA targets in the presence of Mg^{2+} ions. The degradation of hp-51 is extensive, whereas the degradation of the modified DNA target is dramatically reduced. The residual degradation observed for hp-51-T is likely to correspond to the degraded R_p phosphorothioate isomer (see above). The DNA target was designed as a hairpin construct and hence degradation is carried out on double-stranded (ds) DNA from nucleotides 51 to 30 and proceeds on single-stranded (ss) DNA for the rest (Figure 2). Figure 5 shows a ladder of fragments within the dsDNA region, whereas no fragments shorter than 30 nucleotides are observed within the ssDNA region. This finding could indicate that DNA degradation is much faster for ssDNA than for dsDNA as shown by exonuclease studies of RS-p53 (Skalski *et al*., 2000; Bakhanashvili, 2001). It is also possible that this pattern is related to the ability of p53 to act as a processive enzyme on the long ssDNA region, as shown again for RS-p53 (Skalski *et al*., 2000). The accumulation of certain intermediates within the dsDNA region (Figure 5) suggests that DNA degradation did not proceed evenly but rather 'stumbled' at two zones located within nucleotides 45–43 and 35–33. As these sites are close to the centers of the two

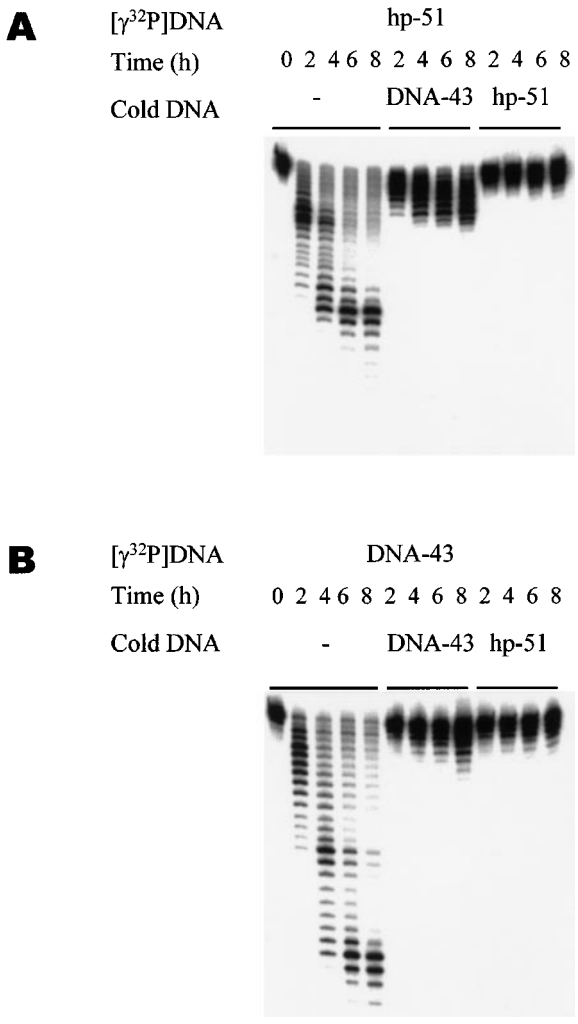

Figure 6 Competition in DNA degradation between the sequence-specific p53 target (hp-51, sequence IIIa) and a non-specific sequence, DNA-43. (**a**) Radioactively labeled hp-51 sequence in the presence of either unlabeled DNA-43 (middle panel) or unlabeled hp-51 (right panel) as a competitor. (**b**) Radioactively labeled DNA-43 sequence in the presence of either unlabeled DNA-43 (middle panel) or unlabeled hp-51 (right panel) as a competitor. Both DNA targets are within intramolecular hairpin constructs with 22 base pairs (hp-51) or 19 base pairs (DNA-43) in the double-stranded stem. 0.5 nM labeled oligonucleotide, 5 nM AS-p53 protein and 170 nM unlabeled competing DNA were used in each experiment. The concentration of AS-p53 in this experiment is 100-fold less than in the other experiments (Figures 4 and 5) to allow the competing DNA to be in molar excess over both the labeled DNA and the protein (see text for details)

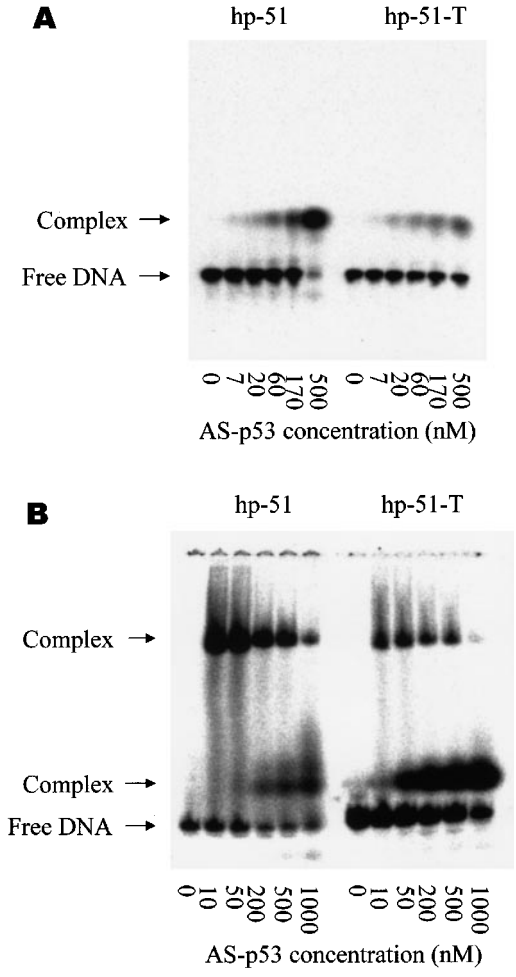

Figure 7 Band-shift analysis of AS-p53 bound to natural and modified DNA targets. (**a**) The single binding mode of AS-p53 interaction with its target site. (**b**) The dual binding mode of AS-p53 interaction with its target site (see the text for details). In both experiments the DNA target is either hp-51 (left panel) or the phosphorothioate analogue hp-51-T (right panel). The DNA concentration is 0.5 nM

decameric binding sites, such observation may be related to the stability of sequence-specific protein-DNA interactions formed by p53 tetramers and dsDNA that are in equilibrium with non-specific protein-DNA interactions formed by p53 monomers and ssDNA (see Discussion).

A competition between the degradation of the specific target (hp-51) and a non-specific hairpin-loop sequence (referred to as DNA-43, see Materials and methods) was performed. Figure 6a illustrates the digestion pattern of labeled hp-51 in the presence of an excess of either cold DNA-43 or cold hp-51, and Figure 6b shows the analogous pattern of labeled DNA-43 in the presence of the same cold DNA sequences. The time points for this experiment are longer than those of Figures 4 and 5, because the protein concentration used in this experiment is reduced by 100-fold (500 nM versus 5 nM respectively). We had to decrease the protein concentration by 100-fold to enable the addition of a molar excess of competitor DNA (170 nM) over the amount of AS-p53 used in the experiment. As a result, the protein concentration was below the K_d value of the enzyme-substrate complex (see below), and therefore the incubation time had to be increased accordingly. The data show that both targets are degraded by AS-p53 but that the sequence-specific DNA target is degraded more efficiently than the non-specific DNA target, because hp-51 competes better than DNA-43 for the radioactively labeled DNA target as shown in Figure 6. Hence, susceptibility to DNA degradation by the protein's enzymatic activity is positively correlated with the stability of the protein-DNA complex.

AS-p53 binding to natural and modified DNA targets

The binding experiments performed with the natural and modified DNA targets (hp-51 and hp-51-T) yielded two distinct binding patterns. In the first pattern, referred to as the single binding mode (Figure 7a), a single shifted band close to the free DNA band appears at protein concentration around 20 nM and grows in intensity as the protein concentration is increased. In the second pattern, referred to as the dual binding mode (Figure 7b), a low mobility band is observed at protein concentration around 10 nM and disappears at higher protein concentration, while a second band of higher mobility and close to the free DNA band appears at protein concentration greater than 10 nM. The second band grows in intensity at the expense of the first band, eventually absorbing most of the labeled material (Figure 7b). The position of this high-mobility band is similar to that of the single band in the other binding pattern. The two DNA binding patterns, a single shifted band versus two shifted bands, were obtained from the same protein preparations. The difference appears to be related to the protein's storage conditions. Whereas the two-band patterns were obtained with freshly prepared protein samples, the single-band gel shifts were obtained mostly when the purified protein was stored at -80°C and thawed at 4°C prior to the binding reaction. This indicates that the protein underwent a transition from one oligomeric form to another as a result of freezing and thawing.

The appearance of the shifted bands close to the free DNA in either pattern is very diffuse and, for the natural sequence, also occasionally smeared (Figure 7b). This raises several possibilities regarding its identity. The possibility of protein degradation in the presence of DNA, as reported by Milner and coworkers (Molinari *et al*., 1996; Okorokov and Milner, 1999), was examined by incubating AS-p53 with its DNA target at various protein/DNA concentrations. The SDS gels of the protein/DNA mixture as a function of time did not indicate the presence of protein degradation products (data not shown). Another possibility is that the high-mobility band is another free DNA entity with a reduced mobility, induced in the presence of high protein levels. To test this, the experiment was repeated with a 100-fold larger concentration of cold DNA (50 nM) in order to increase the amount of the shifted protein, and the gel was silver stained. The free DNA bands were beyond the detection limit of this method, whereas the bands corresponding to the presumed p53-DNA complex were visible at the same position as that of the bands on the radioactive gel, thus confirming the presence of protein in the higher-mobility bands (data not shown). The complete conversion from the upper band to the lower band as the protein concentration is increased, and the high purity of AS-p53 (better than 95%), rule out the possibility that the lower band is caused by an unrelated contaminating protein competing with p53 for DNA binding.

As pointed out previously, the high-mobility bands in all the binding experiments are diffuse regardless of the nature of the DNA target. This observation could indicate that the population of the corresponding protein-DNA species is heterogeneous due to conformational alterations in either interacting component or both. As a consequence of the respective high and low susceptibilities of the natural and of the modified DNA to degradation by AS-p53, differences between the band-shift patterns of the two targets are observed. The free DNA appears as multiple smeared bands in the band-shift experiments with the natural target whereas the gels with the modified DNA target exhibit a single free DNA band (Figures 3 and 7). The high-mobility shifted band of the natural target shown in Figure 7B appears highly smeared whereas the equivalent band shown by the modified sequence is much less so and of much higher intensity. Moreover, the amount of radioactivity at the right-most lane of the natural target contains only a fraction of the total radioactivity of the other lanes. This loss is a consequence of DNA degradation to nucleotides that run out of the gel. In contrast, the amounts of radioactivity in the lanes corresponding to the modified DNA target are similar. We therefore suggest that the high-mobility protein-DNA bands are the ones associated with the protein's exonuclease-compatible

conformation. The observation that the 'tail' of the smear in the high mobility band is pointing upward (Figure 7b) is a consequence of the heterogeneity of the protein-DNA complexes due to DNA fragmentation. Smaller DNA fragments are of smaller negative charge and hence the corresponding protein-DNA complex would be of lower mobility. This pattern should be contrasted with the smear associated with the low-mobility upper band. The downward pointing smear at the two lowest protein concentration lanes reflects a certain instability of the protein-DNA complex under the gel running conditions. As the complex migrates through the gel, it occasionally dissociates producing free DNA that migrates faster than the complex. The smear above this band is probably due to higher-order p53-DNA complexes. Another significant observation is that the low mobility bands of hp-51 are much more intense than those of hp-51-T (Figure 7b) indicating a higher binding affinity of AS-p53 to hp-51 than to hp-51-T. Although the modification is located outside the consensus motif of the DNA sequence (IIIb in Figure 2), its close location to the specific DNA region may interfere with binding, resulting in diminished affinity.

Discussion

In this study we have characterized the binding properties and exonuclease activity of AS-p53 in an attempt to gain insight into the structural/functional role of this naturally occurring p53 variant. AS-p53 differs from RS-p53 in several functional aspects, as outlined in the introduction. The C-terminus of RS-p53 plays a central role in controlling its function. AS-p53 offers an important physiological model in attempts to decipher the specific role of this domain.

AS-p53 binds sequence-specifically to its DNA target under conditions where RS-p53 requires activation such as by binding to specific antibodies (Wu *et al*., 1994; Wolkowicz *et al*., 1995). The requirement for RS-p53 activation in DNA binding studies was attributed to the negative regulatory effect of its extreme C-terminus. Two models were proposed to explain this phenomenon: the allosteric hypothesis, where a transition from a latent p53 conformation to an active conformation is required for sequence-specific binding (Halazonetis and Kandil, 1993; Hupp and Lane, 1994), and the interference hypothesis proposing that non-specific DNA molecules, used in the binding experiments, interact non-specifically with the protein's C-terminus, thereby interfering with p53 sequence-specific DNA binding (Bayle *et al*., 1995; Anderson *et al*., 1997). These ideas are further supported by two recent studies on bacterially produced RS-p53. The first study showed that RS-p53 binds readily to its sequence-specific DNA target without activation, but in the presence of a large excess of non-specific competitor DNA this binding requires activation (Nichols and Matthews, 2001). In the second study, a dimeric p53 protein with an intact C-terminus was also shown to bind to its DNA target in the absence of non-specific competitor DNA, although its binding affinity was lower than that of the C-terminus truncated protein (Ayed *et al*., 2001). In addition, the NMR spectra of the two dimeric proteins were indistinguishable, suggesting that the 'latent' and 'active' proteins adopt similar conformations in the absence of DNA (Ayed *et al*., 2001). However, other recent data suggest positive regulation by the p53 C-terminus when the specific DNA target is embedded within long nonspecific DNA or in chromatin (Espinosa and Emerson, 2001).

The conflicting results from the various DNA binding experiments point to the possibility that the nature of the particular assay affects the DNA binding data, and hence the role of the C-terminus in regulating sequence-specific DNA binding (Ahn and Prives, 2001). It may well be that the role of the C-terminus is more complex than previously anticipated, and it can act either as a negative or a positive regulator depending on the specific DNA and the particular experimental settings that could mimic various physiological conditions. In this respect, the role of the alternatively spliced C-terminus of p53 is very intriguing as it provides yet another mean to regulate p53 function.

The bacterially produced AS-p53 protein of the present study is similar to the *in vitro* translated protein in that it binds sequence specifically to its DNA response elements either in the presence or in the absence of competitor DNA. Our data show however that AS-p53 exhibits two different binding modes. The corresponding protein-DNA complexes are likely to represent different conformations of both the protein and the DNA target, associated with distinct oligomeric states. Although the dominant oligomeric state of the purified free AS-p53 used in our experiments could be either a dimer or a tetramer as indicated by gel filtration chromatography, this is not necessarily the oligomeric state of the protein when bound to DNA. Other oligomeric forms of higher or lower molecular weights can be formed with the DNA, depending on the specific binding mode. In the binding pattern shown in Figure 7b, the slow-migrating protein-DNA complex is likely to be an AS-p53 tetramer bound to dsDNA, whereas the rapid-migrating form is probably a protein monomer bound to ssDNA (see below). The transition from one oligomeric form to another is induced by an increase in the protein concentration. The first form is dominant at the nanomolar concentration range of AS-p53 and the second form at the micromolar range. In other words, the equilibrium between the two forms is shifted from the tetrameric form toward the monomeric form as the total protein concentration is increased. This phenomenon may be related to the observation that p53 monomers, rather than higher oligomers, bind to single-stranded DNA (Skalski *et al*., 2000). As the total protein concentration is raised, the fraction of p53 monomers that bind non-specifically to single-stranded DNA (e.g. at the loop region) is increased, thereby initiating duplex dissociation as well as steric inter-

ference. As a result, the equilibrium between the double-stranded and the single-stranded conformations is shifted gradually toward the latter, and hence tetrameric p53 is excluded from binding to DNA and the monomeric form dominates. The observation that the C-terminus of RS-p53 has the capacity to promote reassociation of single-stranded RNA or DNA into duplex structures, whereas the C-terminus of AS-p53 does not have this capacity (Wu *et al*., 1995), further supports the above model for AS-p53.

It is reasonable to assume that the two species have different functional roles. Whereas the high-affinity complex could be important for activating p53 target genes, the transition to the low-affinity complex could provide a mechanism for controlling such activity at higher protein levels. Moreover, since the high-mobility/low-affinity complex is associated with DNA degradation as shown above, we suggest that it represents the exonuclease-activated form of AS-p53 that could play a specific role in the presence of damaged DNA, as discussed below. It should be pointed out that on the basis of photoaffinity labeling of RS-p53, Skalski *et al*. (2000) proposed that p53 functions as an exonuclease in its monomeric state, which is in agreement with the present findings on AS-p53.

Deppert and coworkers, who discovered the ability of p53 to act as an exonuclease, have shown that this activity is mediated by the p53 DNA binding domain (Mummenbrauer *et al*., 1996; Janus *et al*., 1999). They related this finding to the structural similarity between this domain and the catalytic domain of *E. coli* exonuclease III (Mummenbrauer *et al*., 1996; Janus *et al*., 1999). By performing elaborately systematic studies on various p53 variants, they found that truncation of the last 30 amino acids from the C-terminus of RS-p53 increased the exonuclease activity. However, other means of activating sequence-specific DNA binding such as monoclonal antibodies that recognize the C-terminal epitope of p53 or a higher phosphorylation state inhibited the exonuclease activity of full-length p53. Based on these findings it was proposed that the two activities are mutually exclusive (Albrechtsen *et al*., 1999).

DNA binding and exonuclease activity of AS-p53 appear to be positively correlated based on the following: (i) extensive DNA degradation is observed in the binding experiments with the natural target and (ii) the sequence-specific DNA target is more efficiently degraded by AS-p53 than a non-sequence-specific DNA. Since DNA degradation by AS-p53 is observed only for the low-affinity protein/DNA complexes, it appears that the high-affinity DNA binding mode and exonuclease activity of this protein are mutually exclusive. However, sequence-specific binding of AS-p53 tetramers ensures that there is a large pool of p53 readily available to proceed with exonucleolytic activity when DNA nicks are encountered at the vicinity of p53 binding sites. According to the present model, DNA degradation is caused by the exonucleolytic activity of p53 monomers which are in equilibrium with p53 tetramers that lack this activity. As DNA digestion proceeds, the availability of sequence-specific p53 binding sites is diminished. As a result, the equilibrium is shifted from tetrameric p53 complexes to monomeric p53 complexes, thereby driving an 'autocatalytic' cycle until DNA degradation is complete. Such arguments could explain our findings on enhanced degradation of sequence-specific targets relative to non-specific DNA sequences as well as its 'stumbling' at the nucleotide sites that constitute the centers of the two decameric binding sites (see Results). Since the dissociation rate of tetramers to monomers is dependent on the nature of the C-terminus that incorporates the oligomerization domain, it stands to reason that modifications in this domain by various ways (e.g. alternative splicing, deletion, phosphorylation) regulate the protein's exonuclease activity as found for RS-p53 (Albrechtsen *et al*., 1999).

Janus *et al*. (1999) proposed that wild type RS-p53 is involved in DNA damage repair, or in the control of homologous recombination through its exonuclease activity. This is supported by observations that RS-p53 enhanced the fidelity of DNA replication by DNA polymerase α (Huang, 1998), and the formation of a stable complex between the two proteins (Kuhn *et al*., 1999). It was also observed that the human recombinase hRad51 stimulates exonucleolytic DNA degradation by p53, mediated by the ternary complex p53/hRad51/ junction DNA, thus suggesting a model for p53-dependent correction of DNA exchange events (Susse *et al*., 2000). More recently, it has been shown that RS-p53 can enhance base excision repair *in vitro* and that both the N-terminal transactivation domain and the central DNA binding domain are required to stimulate this activity (Offer *et al*., 1999, 2001; Zhou *et al*., 2001). This activity correlated with the protein's ability to interact directly with the AP endonuclease and with DNA polymerase β (Zhou *et al*., 2001). It still remains to be seen whether AS-p53 has a similar capacity to enhance such activities.

AS-p53 is preferentially expressed in the G2 phase of the cell cycle (Kulesz-Martin *et al*., 1994). This is the checkpoint for detecting errors in the replicated genome prior to mitosis (Schwartz and Rotter, 1998) and it is therefore likely that AS-p53 acts as an exonuclease in concert with other proteins like those involved in DNA synthesis and repair. However, based on our observation that AS-p53 exonuclease activity is positively correlated with its DNA binding affinity together with our proposed model for its mode of action, it is tempting to speculate that AS-p53 may act as an independent exonuclease *in vivo* for rapid degradation of damaged DNA (e.g., nicks and gaps) at the vicinity of DNA control regions containing p53 response elements. Such specific activity would block aberrant p53-dependent signaling pathways. Additional biophysical and functional studies of the alternatively spliced p53 in relation to other p53 variants are needed to gain insight into the specific role of this molecule in the cell.

Materials and methods

Production and purification of p53

Recombinant AS-p53 was produced in *E. coli* BL21(DE3) cells using a pET-21a vector (Shohat-Foord *et al*., 1991). Freshly transformed cells were grown to $A_{560}=0.6-0.8$ and induced with 0.4 mM of IPTG. The cells were harvested after 4 h of induction, re-suspended in a buffer containing 20 mM Tris-HCl pH 8.0, 50 mM NaCl, 1 mM EDTA, 10% glycerol, 5 mM DTT, 0.5 mM PMSF, 0.1 unit/ml aprotinin, and 10 μg/ml pepstatin A and extensively sonicated. The insoluble fraction was collected by centrifugation, washed with the same buffer and then resuspended by trituration in 8 M Urea containing 20 mM Tris-HCl pH 8.0 and 5 mM DTT. After centrifugation the supernatant was dialyzed against a buffer containing 20 mM Tris-HCl pH 8.0, 10% glycerol, 5 mM DTT, 50 mM NaCl, and 0.1 mM $ZnCl_2$. The fractions were confirmed to contain p53 by Western analysis using pAB-anti AS (Wolkowicz *et al*., 1995) and the corresponding SDS gels are shown in Figure 1a. The protein solution was then loaded on a DEAE-Sepharose column equilibrated with the same buffer and eluted with a step gradient of 0.5 M NaCl. The pooled p53-containing fraction was concentrated to approximately 5 mg/ml of total protein by a Schleicher and Schuell concentrator (75 kDa cutoff). Gel filtration chromatography at this stage showed two major peaks of AS-p53, one corresponding to a molecular weight larger than 1000 kD and the other to a molecular weight close to 120 kD (Figure 1b). The lower molecular weight component was collected and loaded on an ion exchange column (Mono Q Pharmacia) using a shallow NaCl gradient and eluted at nearly 200 mM NaCl. No transition to higher aggregates was observed in the course of several days. All procedures were performed at 4°C. An identical procedure was used to produce AS-p53 carrying the point mutation Cys132Phe (referred to as M8-p53) that is deficient in DNA binding (Wolf *et al*., 1985; Arai *et al*., 1986). The identity of the proteins was confirmed by amino acid analysis. The purity of the final preparations was better than 95% according to a silver-stained SDS polyacrylamide gel (Figure 1c). Protein concentration was determined by the Bradford assay (Biorad) with BSA as a standard. The purified protein samples were used directly in the experiments described below or aliquoted and stored at -80°C.

DNA binding experiments

DNA binding to AS-p53 was studied by the electrophoretic mobility shift assay (EMSA). Oligonucleotides were synthesized on an automatic synthesizer and purified by denaturing gel electrophoresis using published procedures (Sambrook *et al*., 1989). All sequences were end-labeled with γ-^{32}P-ATP and polynucleotide kinase, and then purified either on a denaturing gel or by passing them several times through a spin column, as described by Sambrook *et al*. (1989). After re-suspension in TE buffer (10 mM Tris-HCl, pH 8, 1 mM EDTA), the purified hairpin constructs were heated at 90°C for 10 min and flash cooled on ice, whereas the linear double-stranded oligonucleotides were hybridized by heating to 90°C for 10 min and slow cooling the solution to room temperature overnight.

Binding reactions were performed in 10 μl samples, which were incubated for 30 min at 4°C. The reaction mixture included labeled oligonucleotide (0.5 nM) and protein at designated concentrations in a binding buffer containing 20 mM Tris-HCl pH 8.0, 2.5 mM $MgCl_2$, 200 mM NaCl, 0.1 mM $ZnCl_2$, 5 mM DTT, 0.1% NP40 and 10% glycerol. After incubation, the mixture was loaded on native gels (6%, 75:1 acrylamide:bisacrylamide ratio, 10% glycerol) in a 10 mM Na-Phosphate buffer pH 5.5, while the gel was running. The gels were run at 400 V at constant temperature (19°C) with constant buffer circulation until the bromophenol blue dye migrated 10 cm on 15 cm gel. The dried gels were exposed to Fuji or Molecular Dynamics imaging plates.

3′-5′ Exonuclease activity measurements

The p53 binding sites used in these experiments were sequences I, IIIa and IIIb (Figure 2). The non-specific sequence (DNA-43) used in the competition experiments is a hairpin construct of the sequence 5′-GGGCTATAAA-AGGGGGTGGCCCCCCCACCCCCTTTTATAGCCC. All sequences were end-labeled as for the DNA binding experiment and then purified on a denaturing gel. Sequence I was also labeled by dGTP, [α-^{32}P]dATP, dTTP and the Klenow enzyme and then passed through a spin column (Sambrook *et al*., 1989) resulting in the addition of a radioactive adenine nucleotide at the 3′-end of each strand. The reaction mixtures for these experiments contained labeled DNA (0.5 nM), AS-p53 (5 or 500 nM) in a binding buffer containing 20 mM Tris-HCl pH 8.0, 200 mM NaCl, 5 mM DTT, 0.1% NP40 and 10% glycerol, in the presence of various divalent ions. The concentration of cold DNA used in the competition experiments was 0.17 μM. Aliquots (10 μl each) from the reaction mixture were taken at measured time intervals and the reaction was stopped by the addition of 10 mM EDTA and 0.1% SDS. The samples were incubated at 90°C for 10 min followed by flash cooling on ice. After phenol-chloroform extraction and ethanol precipitation in the presence of 10 μg glycogen, the samples were run on 10 or 16% denaturing gels. The gels were dried and exposed to an imaging plate.

Acknowledgments
We thank Professor Don Crothers for helpful comments on the manuscript. The work was supported by grants from the MINERVA Foundation, the Kimmelman Center for Macromolecular Assemblies, the United States–Israel Binational Science Foundation, the Israel Cancer Society and the J and A Taub Biological Research Fund. V Rotter is the incumbent of the Norman and Helen Asher Professorial Chair in Cancer Research and Z Shakked is the incumbent of the Helena Rubinstein Professorial Chair in Structural Biology.

References

Ahn J and Prives C. (2001). *Nature Struct. Biol.*, **8,** 730–732.
Albrechtsen N, Dornreiter I, Grosse F, Kim E, Weismuller L and Deppert W. (1999). *Oncogene,* **18,** 7706–7717.
Almog N, Goldfinger N and Rotter V. (2000). *Oncogene,* **19,** 3395–3403.
Almog N and Rotter V. (1997). *Biochim. Biophys. Acta,* **1333,** F1–F27.
Anderson ME, Woelker B, Reed M, Wang P and Tegtmeyer P. (1997). *Mol. Cell Biol.*, **17,** 6255–6264.

Arai N, Nomura D, Yokota K, Wolf D, Brill E, Shohat O and Rotter V. (1986). *Mol. Cell. Biol.,* **6,** 3232–3239.
Ayed A, Mulder FAA, Yi G-S, Lu Y, Kay LE and Arrowsmith CH. (2001). *Nature Struct. Biol.,* **8,** 756–760.
Bakhanashvili M. (2001). *Eur. J. Biochem.,* **268,** 2047–2054.
Bayle JH, Elenbaas B and Levine AJ. (1995). *Proc. Natl. Acad. Sci. USA,* **92,** 5729–5733.
Brautigam CA and Steitz TA. (1998). *J. Mol. Biol,* **277,** 363–377.
Eckstein F. (1985). *Annu. Rev. Biochem.,* **54,** 367–402.
El-Deiry WS, Kern SE, Pietenpol JA, Kinzler KW and Vogelstein B. (1992). *Nature Gen.,* **1,** 45–49.
Espinosa JM and Emerson BM. (2001). *Mol. Cell.,* **8,** 57–69.
Funk WD, Pak DT, Karas RH, Wright WE and Shay JW. (1992). *Mol. Cell. Biol.,* **12,** 2866–2871.
Giaccia AJ and Kastan MB. (1998). *Genes Dev.,* **12,** 2973–2983.
Hainaut P and Hollstein M. (2000). *Adv. Cancer Res.,* **77,** 81–137.
Hainaut P, Soussi T, Shomer B, Hollstein M, Greenblatt M, Hovig E, Harris CC and Montesano R. (1997). *Nucleic Acids Res.,* **25,** 151–157.
Halazonetis TD and Kandil AN. (1993). *EMBO J.,* **12,** 5057–5064.
Han KA and Kulesz-Martin MF. (1992). *Nucleic Acids Res.,* **20,** 1979–1981.
Haran TE, Joachimiak A and Sigler PB. (1992). *EMBO J.,* **11,** 3021–3030.
Huang P. (1998). *Oncogene,* **17,** 261–270.
Hupp TR and Lane DP. (1994). *Curr. Biol.,* **4,** 865–875.
Janus F, Albrechtsen N, Knippschild U, Wiesmuller L, Grosse F and Deppert W. (1999). *Mol. Cell. Biol.,* **19,** 2155–2168.
Jayaraman L and Prives C. (1999). *Cell. Mol. Life Sci.,* **55,** 76–87.
Ko J and Prives C. (1996). *Genes Dev.,* **10,** 1054–1072.
Kuhn C, Muller F, Melle C, Nasheuer HP, Janus F, Deppert W and Grosse F. (1999). *Oncogene,* **18,** 769–774.
Kulesz-Martin MF, Lisafeld B, Huang H, Kisiel ND and Lee L. (1994). *Mol. Cell. Biol.,* **14,** 1698–1708.
Levine AJ. (1997). *Cell,* **88,** 323–331.
Longley MJ and Mosbaugh DW. (1991). *J. Biol. Chem.,* **266,** 24702–24711.
May P and May E. (1999). *Oncogene,* **18,** 7621–7636.
Molinari M, Okorokov AL and Milner J. (1996). *Oncogene,* **13,** 2077–2086.
Mummenbrauer T, Janus F, Muller B, Wiesmuller L, Deppert W and Grosse F. (1996). *Cell,* **85,** 1089–1099.
Nichols NM and Matthews KS. (2001). *Biochemistry,* **40,** 3847–3858.
Offer H, Milyavsky M, Erez N, Matas D, Zurer I, Harris CC and Rotter V. (2001). *Oncogene,* **20,** 581–589.
Offer H, Wolkowicz R, Matas D, Blumenstein S, Livneh Z and Rotter V. (1999). *FEBS Lett.,* **450,** 197–204.
Okorokov AL and Milner J. (1999). *Onc. Res.,* **9,** 267–273.
Oren M. (1999). *J. Biol. Chem.,* **274,** 36031–36034.
Ryan KM, Phillips AC and Vousden KH. (2001). *Curr. Opin. Cell. Biol.,* **13,** 332–337.
Sambrook J, Fritsch EF and Maniatis T. (1989). *Molecular cloning. A laboratory manual.* 2nd Ed. Cold Spring Harbor, NY: Cold Spring Harbor Laboratory.
Schwartz D and Rotter V. (1998). *Semin. Cancer Biol.,* **8,** 325–336.
Shohat-Foord O, Bhattacharya P, Reich Z and Rotter V. (1991). *Nucleic Acids Res.,* **19,** 5191–5198.
Skalski V, Lin Z-Y, Choi BY and Brown KR. (2000). *Oncogene,* **19,** 3321–3329.
Susse S, Janz C, Janus F, Deppert W and Wiesmuller L. (2000). *Oncogene,* **19,** 4560–4512.
Wang XW and Harris CC. (1997). *J. Cell Physiol.,* **173,** 247–255.
Wolf D, Harris N, Goldfinger N and Rotter V. (1985). *Mol. Cell. Biol.,* **5,** 127–132.
Wolkowicz R, Peled A, Elkind NB and Rotter V. (1995). *Proc. Natl. Acad. Sci. USA,* **92,** 6842–6846.
Wolkowicz R and Rotter V. (1997). *Path. Biol.,* **45,** 785–796.
Wu L, Bayle JH, Elenbaas B, Pavletich NP and Levine AJ. (1995). *Mol. Cell. Biol.,* **15,** 497–504.
Wu Y, Liu Y, Lee L, Miner Z and Kulesz-Martin M. (1994). *EMBO J.,* **13,** 4823–4830.
Zauberman A, Barak Y, Ragimov N, Levy N and Oren M. (1993). *EMBO J.,* **12,** 2799–2808.
Zhou J, Ahn J, Wilson SH and Prives C. (2001). *EMBO J.,* **20,** 914–923.